



Analytical and experimental studies on the thermal performance of cross-corrugated and flat-plate solar air heaters

Wenfeng Gao ^a, Wenxian Lin ^{a,b,*}, Tao Liu ^a, Chaofeng Xia ^a

^a *Solar Energy Research Institute, Yunnan Normal University, Kunming 650092, People's Republic of China*

^b *School of Engineering, James Cook University, Townsville, Qld. 4811, Australia*

Received 4 November 2005; received in revised form 18 February 2006; accepted 25 February 2006

Abstract

The cross-corrugated heaters consist of a wavelike absorbing plate and a wavelike bottom plate, which are crosswise positioned to form the air flow channel. Two types of these heaters are considered. For the type 1 heater, the wavelike shape of the absorbing plate is along the flow direction and that of the bottom plate is perpendicular to the flow direction, while for the type 2 heater it is the wavelike shape of the bottom plate that is along the flow direction and that of the absorbing plate is perpendicular to the flow direction. The aims of the use of the cross-corrugated absorbing plate and bottom plate is to enhance the turbulence and the heat-transfer rate inside the air flow channel, which are crucial to the improvement of efficiencies of solar air-heaters. To quantify the achievable improvements with the cross-corrugated absorbing and bottom plates, flat-plate solar air-heaters which have both a flat absorbing plate and a flat bottom plate, are also considered. The thermal performance of these three types of solar air-heaters are analyzed, measured and compared under several configurations and operating conditions. All the analytical and experimental results show that, although the thermal performance of the type 2 heater is just slightly superior to that of the type 1 heater, both of these cross-corrugated solar air-heaters have a much superior thermal performances to that of the flat-plate one. It is also found that the use of selected coatings on the absorbing plates of all the heaters considered can substantially enhance the thermal performances of the heaters, whereas such a selected coating on the bottom plates or/and the glass covers does not have such a significant effect on the thermal performances of the heaters.

© 2006 Elsevier Ltd. All rights reserved.

* Corresponding author. Address: School of Engineering, James Cook University, Townsville, Qld. 4811, Australia; Tel.: +86 871 5823640; fax: +86 871 5516217.

E-mail address: linwenxian@ynnu.edu.cn (W. Lin).

Keywords: Cross-corrugated solar air heater; Thermal performance; Analytical solution; Experimental results; Wavelike absorbing-plate; Wavelike bottom-plate

1. Introduction

Solar air-heaters are key components in many engineering applications, such as in building heating systems, in solar drying-devices, etc. [1,2]. Due to the poor thermal conductivity and small heat capacity of air, the convective heat-transfer rate inside the air flow-channel where the air is heated is low, and a great deal of effort has been made to increase this rate [3]. One of the effective ways to augment the convective heat-transfer rate is to increase the heat-transfer surface area and to increase the turbulence inside the channel by using fins or corrugated surfaces [4,5] and many studies have been carried out on this topic. For example, the convective heat transfer in a Vee-trough linear solar heater was studied by Meyer et al. [6] while the natural convection in a channel formed by a Vee-shaped surface and a flat plate was studied numerically and experimentally by Zhao and Li [7]. Stasiek [8] carried out experimental studies on the heat transfer and fluid flow across corrugated-undulated heat-exchanger surfaces. Piao et al. [9,10] investigated experimentally natural, forced and mixed convective heat-transfers in a cross-corrugated channel solar air-heater. Noorshahi et al. [11] conducted a numerical study on the natural convection in a corrugated enclosure with mixed boundary-conditions. Gao et al. [12,13] numerically simulated the natural convection inside the channel formed by a flat cover and a wavelike absorbing plate.

In this paper, analytical and experimental studies have been carried out to investigate the thermal performances of cross-corrugated solar air-heaters in which the wavelike shapes of the absorbing plate and the bottom plate are perpendicular to each other and the air flows through the channel formed by these two plates and to compare with those of flat-plate solar air-heaters, where both the absorbing plate and the bottom plate are flat, to show the efficiency improvement achievable with the use of the cross-corrugated absorbing plate and bottom plate.

2. Theoretical analysis

Two types of cross-corrugated solar air heaters are considered in this paper. Both types consist of a single flat glass-cover, a wavelike absorbing-plate and a wavelike bottom-plate, which is attached to back insulation beneath. The channel formed by the absorbing plate and the bottom plate is the air flow-channel where the air is heated by the absorbed solar radiation on the absorbing plate. In the type 1 heater, as sketched in Fig. 1, the wavelike shape of the absorbing plate is along the air-flow direction and that of the bottom plate is perpendicular to the air-flow direction. In the type 2 heater, however, it is the wavelike shape of the bottom plate that is along the air flow direction and the absorbing plate is perpendicular to the flow direction. The aim of the use of the cross-corrugated absorbing plate and bottom plate, as mentioned above, is to enhance the turbulence and the heat-transfer rate inside the air flow-channel which are crucial to the improvement of efficiencies of solar air heaters. To quantify the achievable improvements with the cross-corrugated absorbing and bottom plates, a flat-plate solar air-heater (referred to as the type 3 heater), which has both a flat absorbing plate and a flat bottom plate, is also analyzed.

Nomenclature

A_c	area of the heater surface (m^2)
c_p	specific heat of air ($J/kg\ K$)
D_h	hydraulic diameter of the air flow-channel (m)
F_0	new heater heat-removal factor
F_R	heater heat-removal factor
g	acceleration due to gravity (m/s^2)
h_b	conduction heat-transfer coefficient across the insulation ($W/m^2\ K$)
$h_{c,ap-c}$	convection heat-transfer coefficient between the cover and the absorbing plate ($W/m^2\ K$)
$h_{c,ap-f}$	convection heat-transfer coefficient of fluid on the absorbing plate ($W/m^2\ K$)
$h_{c,f-ap}$	same as $h_{c,ap-f}$ ($W/m^2\ K$)
$h_{c,f-bp}$	convection heat-transfer coefficient of fluid on the bottom plate ($W/m^2\ K$)
$h_{r,ap-c}$	radiation heat-transfer coefficient between the cover and the absorbing plate ($W/m^2\ K$)
$h_{r,ap-bp}$	radiation heat-transfer coefficient between the absorbing plate and the bottom plate ($W/m^2\ K$)
$h_{r,c-s}$	radiation heat-transfer coefficient between the cover and the sky ($W/m^2\ K$)
h_w	wind convection heat-transfer coefficient ($W/m^2\ K$)
H_c	mean gap-thickness between the cover and the absorbing plate (m)
H_g	mean gap thickness between the absorbing plate and the bottom plate (m)
I	solar insolation rate incident on the glass cover (W/m^2)
k	thermal conductivity of air ($W/m\ K$)
k_i	thermal conductivity of the insulation ($W/m\ K$)
L	heater length (m)
\dot{m}_f	air mass flow-rate per unit area of heater ($kg/m^2\ s$)
Nu_{ap-c}	Nusselt number for the natural convection in the channel formed by the cover and the absorbing plate
Nu_{ap-f}	Nusselt number for the convection of the fluid moving in the air flow-channel
q_u	useful energy gain (W/m^2)
Ra	Rayleigh number
Re	Reynolds number
S	solar radiation absorbed by the absorbing plate per unit area (W/m^2)
T_a	ambient temperature (K)
T_{ap}	mean temperature of the absorbing plate (K)
T_{bp}	mean temperature of the bottom plate (K)
T_c	mean temperature of the glass cover (K)
T_f	mean air temperature (K)
T_{fi}	inlet-air temperature (K)
T_{fo}	outlet-air temperature (K)
T_s	temperature at the sky (K)
\bar{U}_f	mean velocity of fluid in the channel (m/s)
U_L	heater's heat-transfer coefficient ($W/m^2\ K$)
V_w	wind velocity of the ambient air (m/s)
W	heater width (m)

Greek letters

α_{ap}	solar-radiation absorptivity of the absorbing plate
α_c	solar-radiation absorptivity of the glass cover
β	thermal expansion coefficient of air (1/K)
Δ_i	mean thickness of the insulation (m)
ϵ_{ap}	emissivity of thermal radiation of the absorbing plate
ϵ_{bp}	emissivity of thermal radiation of the bottom plate
ϵ_c	thermal-radiation emissivity of the glass cover
η	instantaneous efficiency of solar heat-gain of the heater
θ	angle of inclination of the heater (°)
μ	dynamic viscosity of air (kg/m s)
ρ	density of air (kg/m ³)
σ	Stefan–Boltzmann constant (W/m ² K ⁴)
τ_c	solar-radiation emissivity of the glass cover
$(\tau\alpha)_e$	effective transmittance–absorptance product

To model the heaters considered, a number of simplifying assumptions can be made to lay the foundations without obscuring the basic physical situation. These assumptions are as follows:

- Thermal performance of heaters is steady-state.
- There are a negligible temperature drop through the glass cover, the absorber plate and the bottom plate.
- There is one-dimensional heat-flow through the back insulation, which is in the direction perpendicular to the air flow.
- The sky can be considered as a blackbody for long-wavelength radiation at an equivalent sky-temperature.
- Loss through the front and back are to air at the same ambient temperature.
- Dust and dirt on the heater and the shading of the heater absorbing-plate are negligible.
- Thermal inertia of heater components is negligible.
- Operating temperatures of heater components and mean air-temperatures in the air channels are all assumed to be uniform.
- Temperature of the air varies only in the flow direction.
- All air channels are assumed to be free of leakage.
- Thermal losses through the heater backs are mainly due to the conduction across the insulation: those caused by the wind and the thermal radiation of the insulation are assumed negligible.

2.1. Energy balance equations

The thermal network for all three types of heaters considered in this paper is illustrated in Fig. 2. If the solar-insolation rate incident on the glass cover is I (W/m²), the transmissivity of solar radiation of the glass cover is τ_c , and the absorptivity of solar radiation of the absorbing plate is α_{ap} , the solar radiation absorbed by the absorbing plate per unit

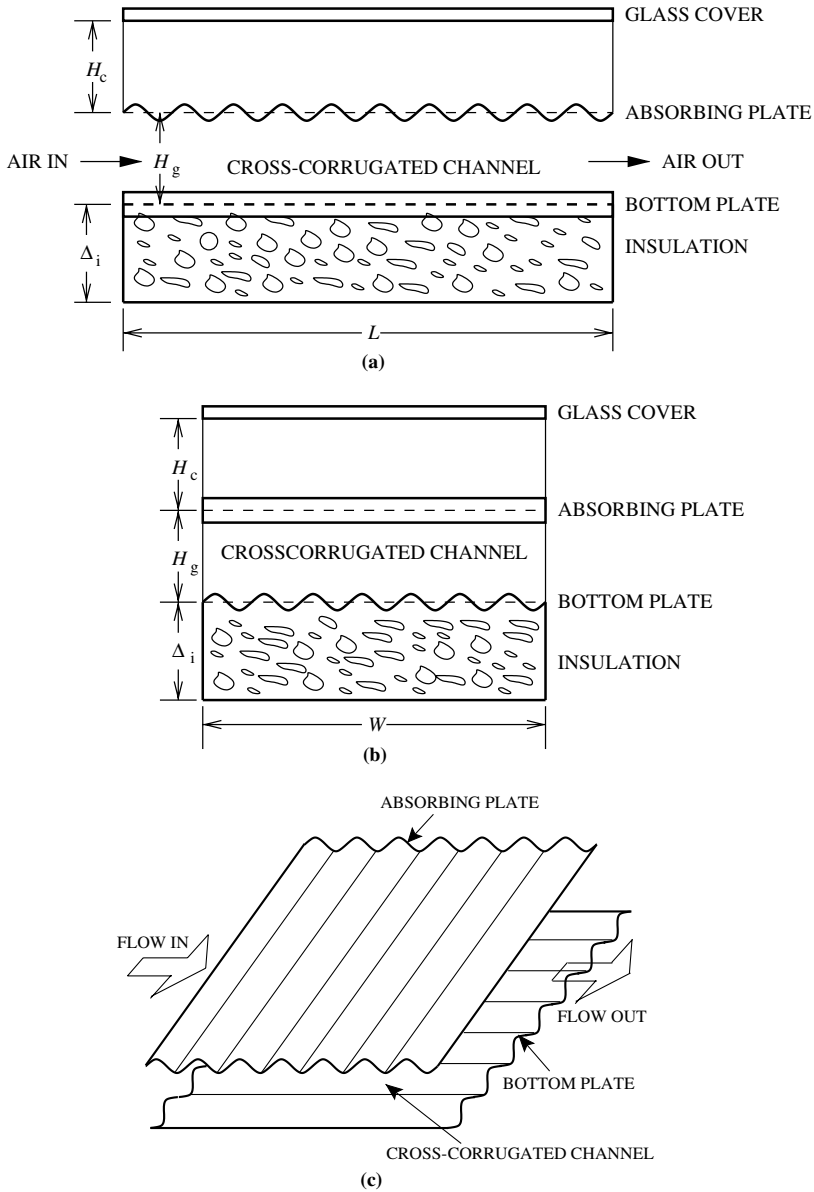


Fig. 1. Schematic description of the type 1 solar air heater which has a cross-corrugated absorbing plate and bottom plate. The wavelike shape of the absorbing plate is along the flow direction and that of the bottom plate is perpendicular to the flow direction. (a) Cross-section view perpendicular to the flow direction; (b) Cross-section view along the flow direction; and (c) Schematic description of the cross-corrugated absorbing plate and bottom plate.

area, S (W/m^2), which is equal to the difference between the incident solar-radiation and the optical loss, is as follows [1]:

$$S \simeq 0.96\tau_c\alpha_{ap}I, \tag{1}$$

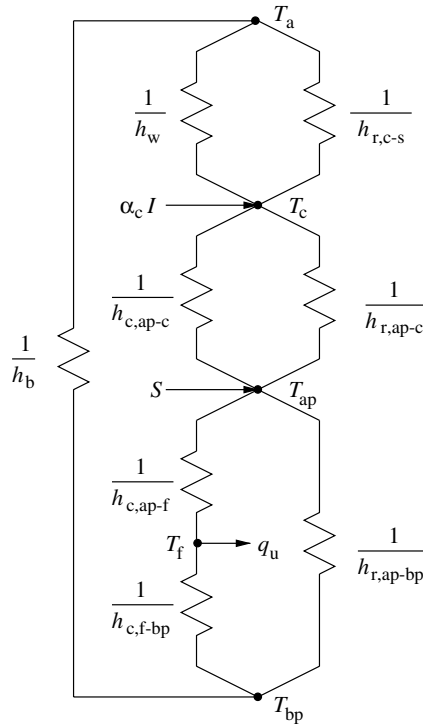


Fig. 2. Thermal network for the single-cover solar air-heater.

where the factor “0.96” represents the averaged transmittance–absorptance product. This absorbed energy S is distributed as thermal losses through the glass cover and the bottom and as useful energy gain q_u (W/m^2) which heats the air in the channel from the inlet temperature T_{fi} (K) to the outlet temperature T_{fo} (K), resulting in the mean air-temperature $T_f = (T_{fi} + T_{fo})/2$.

On the glass cover, the energy gain is $\alpha_c I$, i.e. the solar-radiation absorbed where α_c is the absorptivity of solar radiation by the glass cover; the heat transferred by natural convection from the absorbing plate is represented by $h_{c,ap-c}$ ($\text{W}/\text{m}^2 \text{K}$), which is the convection heat-transfer coefficient between the cover and the absorbing plate; and that transferred by thermal radiation from the absorbing plate represented by $h_{r,ap-c}$ ($\text{W}/\text{m}^2 \text{K}$), which is the radiation heat-transfer coefficient between the cover and the absorbing plate. The energy losses through the glass cover are the heat transferred by convection due to wind represented by h_w ($\text{W}/\text{m}^2 \text{K}$), which is the wind convection heat-transfer coefficient, and that transferred by thermal radiation from the cover to the sky at T_s (K) represented by $h_{r,c-s}$ ($\text{W}/\text{m}^2 \text{K}$) which is the radiation heat-transfer coefficient between the cover and the sky. Hence, the energy balance for the glass cover requires

$$\alpha_c I + (h_{c,ap-c} + h_{r,ap-c})(T_{ap} - T_c) = (h_w + h_{r,c-s})(T_c - T_a), \quad (2)$$

where T_{ap} (K) and T_c (K) are the mean temperature on the absorbing plate and on the surface of the glass cover, and T_a (K) is the ambient temperature.

On the absorbing plate, the absorbed solar radiation S is distributed to thermal losses to the glass cover by natural convection represented by $h_{c,ap-c}$ and by thermal radiation

represented by $h_{r,ap-c}$, to the bottom plate by thermal radiation represented by $h_{r,ap-bp}$, which is the radiation heat-transfer coefficient between the absorbing plate and the bottom plate, and to the fluid by convection represented by $h_{c,ap-f}$ ($W/m^2 K$), which is the convection heat-transfer coefficient of the fluid on the absorbing plate. Hence, the energy balance for the absorbing plate requires

$$S = (h_{c,ap-c} + h_{r,ap-c})(T_{ap} - T_c) + h_{r,ap-bp}(T_{ap} - T_{bp}) + h_{c,ap-f}(T_{ap} - T_f), \tag{3}$$

where T_{bp} (K) is the mean temperature of the bottom plate.

For the fluid, the heat gained from the absorbing plate by convection (represented by $h_{c,ap-f}$) is distributed to the heat gain q_u which is carried away by the fluid and the thermal loss to the bottom plate by convection (represented by $h_{c,f-bp}$ ($W/m^2 K$)) which is the convection heat-transfer coefficient of fluid on the bottom plate, resulting in the following energy-balance:

$$h_{c,ap-f}(T_{ap} - T_f) = q_u + h_{c,f-bp}(T_f - T_{bp}), \tag{4}$$

where $q_u = c_p \dot{m}_f (T_{fo} - T_{fi})$, in which c_p (J/kg K) is the specific heat of air and \dot{m}_f ($kg/m^2 s$) is the air mass flow rate per unit area of heater.

On the bottom plate, the heat gains from the fluid via convection represented by $h_{c,f-bp}$ and from the absorbing plate via thermal radiation represented by $h_{r,ap-bp}$ are balanced by the thermal loss to the ambient environment via conduction represented by h_b ($W/m^2 K$) which is the conduction heat-transfer coefficient across the insulation, that is,

$$h_{r,ap-bp}(T_{ap} - T_{bp}) + h_{c,f-bp}(T_f - T_{bp}) = h_b(T_{bp} - T_a). \tag{5}$$

With the assumption of $T_f = (T_{fo} + T_{fi})/2$, it is found from Eq. (2) that

$$T_c = \frac{\alpha_c I + (h_{c,ap-c} + h_{r,ap-c})T_{ap} + (h_w + h_{r,c-s})T_a}{h_{c,ap-c} + h_{r,ap-c} + h_w + h_{r,c-s}}, \tag{6}$$

from Eq. (3)

$$T_{ap} = \frac{S + (h_{c,ap-c} + h_{r,ap-c})T_c + h_{r,ap-bp}T_{bp} + h_{c,ap-f}T_f}{h_{c,ap-c} + h_{r,ap-c} + h_{r,ap-bp} + h_{c,ap-f}}, \tag{7}$$

from Eq. (4)

$$T_f = \frac{h_{c,ap-f}(T_{ap} + T_{bp}) + 2c_p \dot{m}_f T_{fi}}{2h_{c,ap-f} + 2c_p \dot{m}_f}, \tag{8}$$

and from Eq. (5)

$$T_{bp} = \frac{h_b T_a + h_{r,ap-bp}T_{ap} + h_{c,ap-f}T_f}{h_b + h_{r,ap-bp} + h_{c,ap-f}}. \tag{9}$$

The efficiency of solar heat gain of the heater is

$$\eta = \frac{q_u}{I} = \frac{c_p \dot{m}_f (T_{fo} - T_{fi})}{I} = \frac{2c_p \dot{m}_f (T_f - T_{fi})}{I}. \tag{10}$$

2.2. Determination of heat-transfer coefficients

The convection heat-transfer coefficient from the glass cover due to the wind is recommended by McAdams [14] as

$$h_w = 5.7 + 3.8V_w, \quad (11)$$

where V_w (m/s) is the wind velocity of the ambient air and it is usually assumed that $V_w = 1.5$ m/s [15], which gives $h_w = 11.4$ W/m² K. In this paper, $h_w = 11.4$ W/m² K is also used.

The radiation heat-transfer coefficient from the glass cover to sky the referred to the ambient air temperature T_a (K) may be obtained as follows [15]

$$h_{r,c-s} = \sigma \epsilon_c (T_c + T_s) (T_c^2 + T_s^2) \frac{(T_c - T_s)}{(T_c - T_a)}, \quad (12)$$

where $\sigma = 5.67 \times 10^{-8}$ W/m² K⁴ is the Stefan–Boltzmann constant, ϵ_c is the emissivity of thermal radiation of the glass cover, and the sky temperature T_s (K) is estimated by the formulation given by Swinbank [16],

$$T_s = 0.0552T_a^{1.5}. \quad (13)$$

The radiation heat-transfer coefficients between the glass cover and the absorbing plate and between the absorbing plate and the bottom plate are predicted, respectively, by

$$h_{r,ap-c} = \frac{\sigma(T_{ap}^2 + T_c^2)(T_{ap} + T_c)}{1/\epsilon_{ap} + 1/\epsilon_c - 1}, \quad (14)$$

and

$$h_{r,ap-bp} = \frac{\sigma(T_{ap}^2 + T_{bp}^2)(T_{ap} + T_{bp})}{1/\epsilon_{ap} + 1/\epsilon_{bp} - 1}, \quad (15)$$

where ϵ_{ap} and ϵ_{bp} are the emissivities for thermal radiation of the absorbing plate and the bottom plate.

The conduction heat-transfer coefficient across the insulation is estimated by

$$h_b = \frac{k_i}{\Delta_i}, \quad (16)$$

where k_i (W/m K) is the thermal conductivity of the insulation and Δ_i (m) is the mean thickness of the insulation.

The convection heat-transfer coefficient between the glass cover and the absorbing plate is calculated by

$$h_{c,ap-c} = Nu_{ap-c} \frac{k}{H_c}, \quad (17)$$

where k (W/m K) is the thermal conductivity of air, H_c (m) is the mean gap-thickness between the cover and the absorbing plate as sketched in Fig. 1, and Nu_{ap-c} is the Nusselt number for natural convection in the channel formed by the cover and the absorbing plate.

For the type 1 heater, the following correlation, developed by Zhao and Li [7], can be used to approximate Nu_{ap-c} , i.e.,

$$Nu_{ap-c} = 0.1673(Ra \cos \theta)^{0.2917}, \quad (18)$$

where θ (°) is the angle of inclination of the heater and Ra is the Rayleigh number which is defined as

$$Ra = \frac{\rho^2 c_p g \beta (T_{ap} - T_c) H_c^3}{k \mu}, \quad (19)$$

in which ρ (kg/m³), β (1/K) and μ (kg/m s) are the density, thermal-expansion coefficient and dynamic viscosity of air, and g (m/s²) is the acceleration due to gravity.

For the type 2 and type 3 heaters, Nu_{ap-c} can be estimated by the following correlation [17]

$$Nu_{ap-c} = 1 + 1.44 \left[1 - \frac{1708(\sin 1.8\theta)^{1.6}}{Ra \cos \theta} \right] \left[1 - \frac{1708}{Ra \cos \theta} \right]^+ + \left[\left(\frac{Ra \cos \theta}{5830} \right)^{1/3} - 1 \right]^+, \tag{20}$$

where the “+” symbol in the superscript means that only positive values of the terms in the square brackets are to be used (i.e., use zero if the term is negative). This correlation is valid for $0^\circ \leq \theta \leq 75^\circ$.

The convection heat-transfer coefficients for the fluid moving on the absorbing plate and on the bottom plate, are calculated by

$$h_{c,ap-f} = h_{c,f-bp} = Nu_{ap-f} \frac{k}{D_h}, \tag{21}$$

where $D_h = 2WH_g/(W + H_g)$ (in m) is the hydraulic diameter of the air flow channel formed by the absorbing plate and the bottom plate, W (m) is the heater width, H_g (m) is the mean gap-thickness between the absorbing plate and the bottom plate as sketched in Fig. 1, and Nu_{ap-f} is the Nusselt number for the convection in the air flow channel.

For the type 1 and type 2 heaters, Nu_{ap-f} can be estimated by the following correlation [9,10]

$$Nu_{ap-f} = 0.0743Re^{0.76}, \tag{22}$$

where Re is the Reynolds number, defined as follows:

$$Re = \frac{\rho \bar{U}_f D_h}{\mu}, \tag{23}$$

in which \bar{U}_f (m/s) is the mean velocity of fluid in the channel. This correlation is valid for $3000 \leq Re \leq 50,000$.

For the type 3 heater, however, Nu_{ap-f} is estimated by the following correlation [18]

$$Nu_{ap-f} = 0.0158Re^{0.8}, \tag{24}$$

where Re is the Reynolds number, defined as follows:

$$Re = \frac{2\rho \bar{U}_f H_g}{\mu}, \tag{25}$$

which is for fully-developed turbulent flow in the channel.

When the air temperature T (K) is in the range 280–470 K, the following empirical correlations can be obtained from [19] to estimate the density, thermal conductivity and dynamic viscosity of air:

$$\rho = 3.9147 - 0.016082T + 2.9013 \times 10^{-5}T^2 - 1.9407 \times 10^{-8}T^3, \tag{26}$$

$$k = (0.0015215 + 0.097459T - 3.3322 \times 10^{-5}T^2) \times 10^{-3}, \tag{27}$$

$$\mu = (1.6157 + 0.06523T - 3.0297 \times 10^{-5}T^2) \times 10^{-6}, \tag{28}$$

while constant $\beta = 1/T$ (1/K) and $c_p \approx 1000$ J/kg K can also be assumed.

2.3. Solutions of temperatures and efficiency

It is apparent from Eqs. (6) to (10) that no analytic solutions can be obtained for the temperatures T_c , T_{ap} , T_{bp} , and T_f and the efficiency η as most of the heat transfer coefficients are functions of these temperatures. Hence, the values of these parameters will be obtained numerically by an iteration method. The procedure is first using guessed temperatures to calculate the heat-transfer coefficients, which are then used to estimate new temperatures, and if all these new temperatures are larger than 0.01% from their respective guessed values then these new temperatures will be used as the guessed temperatures for the next iteration and the process will be repeated until all the newest temperatures obtained are within $\pm 0.01\%$ of their respective previous values.

3. Results and discussion

In this section, solutions are first obtained under the typical configurations and operating conditions for all three types of heaters to catch a glimpse of the general thermal-performances of these heaters and the improvements achievable with the use of the cross-corrugated wavelike absorbing and bottom plates with respect to the flat absorbing-plate and bottom plate. The effects of selected coatings used on the absorbing plate, bottom plate, and glass cover are then examined. Finally, analytical solutions are compared with experimental results for some specific cases.

3.1. Results for typical configurations and operating conditions

The following values are used for the parameters for the case (referred to as the Case 1 hereinafter) under the typical configurations and operating conditions: $I = 800 \text{ W/m}^2$, $\theta = 30^\circ$, $W = 1 \text{ m}$, $L = 2 \text{ m}$, $H_g = 0.04 \text{ m}$, $H_c = 0.04 \text{ m}$, $\dot{m}_f = 0.1 \text{ kg/m}^2 \text{ s}$, $T_a = 285 \text{ K}$, $T_{fi} = 295 \text{ K}$, $\Delta_i = 0.05 \text{ m}$, $k_i = 0.025 \text{ W/m K}$, $\epsilon_{ap} = 0.94$, $\epsilon_{bp} = 0.94$, $\epsilon_c = 0.9$, $\alpha_{ap} = 0.95$, $\alpha_c = 0.06$, $\tau_c = 0.84$, and $h_w = 11.4 \text{ W/m}^2 \text{ K}$.

The results for this typical case are listed in Table 1, where it is found that the type 1 and type 2 heaters, which have the cross-corrugated wavelike absorbing plate and bottom plate, are apparently much superior to the type 3 heater which has the flat absorbing-plate and bottom-plate, with efficiencies about 10% higher (58.9%, 60.3%, and 48.6%, respectively, for the type 1, type 2, and type 3 in this specific case), indicating that the use of the cross-corrugated wavelike absorbing plate and bottom plate does significantly improve the thermal performance of a solar air-heater. Apparently this improvement of thermal performance is due to the enhanced heat-transfer rate inside the air flow channel in the type 1 and type 2 heaters, which is about 3.25 times of that in the type 3 heater ($h_{c,ap-f} = 28.6$, 28.6, and 8.8 $\text{W/m}^2 \text{ K}$, respectively, for the type 1, type 2, and type 3 in this specific case), resulting in much lower temperatures on the cover, absorbing plate, and bottom plates, and larger heat-gains for the fluid in the type 1 and type 2 heaters. Although the type 1 heater has a similar thermal performance to the type 2 heater, it is found that the latter performs slightly superior to the former (a 1.3% higher efficiency). In fact, as will be shown subsequently, these conclusions are generally also correct for other cases considered in this paper.

3.2. Effect of selected coatings

In the case considered above, there is no selected coating on any surface of the heaters. However, selected coatings with high absorptivities of solar radiation and low emissivities of thermal radiation have been widely used in practical applications, especially on absorbing plates and glass covers, with the aim of suppressing the thermal-radiation heat-losses. To demonstrate the effect of selected coatings on the solar air heaters considered here, an additional three cases are also analyzed. In the first case (referred to as Case 2 hereinafter), there are selected coatings on the absorbing plates of the heaters and $\epsilon_{ap} = 0.05$ is then used, while all the other parameters have the same values as those used in Case 1. In the second case (referred to as Case 3 hereinafter), there are selected coatings on both the absorbing plates and the bottom plates of the heaters and $\epsilon_{ap} = 0.05$ and $\epsilon_{bp} = 0.05$ are then used while all the other parameters have the same values as those used in Case 1. In the last case (referred to as the Case 4), there are selected coatings on all the absorbing plates, the bottom plates, and the glass covers of the heaters and $\epsilon_{ap} = 0.05$, $\epsilon_{bp} = 0.05$, and $\epsilon_c = 0.05$ are then used while all the other parameters have the same values as those used in Case 1.

The results for these three additional cases are listed in Tables 2–4, respectively. Compared to Case 1, it is found that the use of the selected coatings on the absorbing plates significantly improve the thermal performances of all three types of heaters, with 9.5%, 11.7%, and 17.2% increases of efficiency, respectively, for type 1, type 2, and type 3 heaters. These improvements are due to the tremendous reductions of the thermal-radiation heat-losses from the absorbing plates to the glass covers with $h_{r,ap-c}$ decreased from 5.30, 5.29, and 5.90 W/m² K to 0.31, 0.31, and 0.38 W/m² K, respectively, for type 1, type 2, and type 3 heaters, and those from the absorbing plates to the bottom plates with $h_{r,ap-bp}$ decreased from 5.74, 5.76, and 6.54 W/m² K to 0.33, 0.33, and 0.40 W/m² K, respectively, for type 1, type 2, and type 3 heaters. The temperatures on the absorbing plates are significantly increased, from 311.7, 312.0, and 328.5 K to 316.9, 318.0, and 355.7 K, respectively, for type 1, type 2, and type 3 heaters, but the temperatures on the glass covers and the bottom plates are dramatically reduced, from 291.5, 290.8, and 296.2 K to 286.9, 285.2, and 288.1 K on the glass covers and from 299.5, 299.6, and 309.6 K to 297.7, 297.9, and

Table 1
Results for the typical configurations and operating conditions: Case 1, no selected coating on any surface

Parameter	Type 1	Type 2	Type 3
η	0.5894	0.6028	0.4861
q_u (W/m ²)	471.56	482.24	388.89
T_c (K)	291.49	290.83	296.17
T_{ap} (K)	311.67	312.04	328.48
T_{bp} (K)	299.54	299.65	309.58
T_{fo} (K)	299.72	299.82	298.89
$h_{r,c-s}$ (W/m ² K)	17.65	19.06	12.42
$h_{r,ap-c}$ (W/m ² K)	5.30	5.29	5.90
$h_{c,ap-c}$ (W/m ² K)	1.66	0.82	0.85
$h_{r,ap-bp}$ (W/m ² K)	5.74	5.76	6.54
$h_{c,ap-f}$ (W/m ² K)	28.59	28.60	8.80
Ra	1,17,836	1,24,080	1,60,326
Re	10,489	10,488	10,500
Nu_c	4.84	2.40	2.41
Nu_f	84.48	84.47	26.04

Table 2

Results for the typical configurations and operating conditions: Case 2, only the absorbing plate has a selected coating

Parameter	Type 1	Type 2	Type 3
η	0.6847	0.7194	0.6586
q_u (W/m ²)	547.72	575.56	526.89
T_c (K)	286.88	285.25	288.11
T_{ap} (K)	316.89	317.99	355.71
T_{bp} (K)	297.74	297.88	299.38
T_{fo} (K)	300.48	300.76	300.27
$h_{r,c-s}$ (W/m ² K)	48.83	324.58	31.41
$h_{r,ap-c}$ (W/m ² K)	0.31	0.31	0.38
$h_{c,ap-c}$ (W/m ² K)	1.86	0.83	0.88
$h_{r,ap-bp}$ (W/m ² K)	0.33	0.33	0.40
$h_{c,ap-f}$ (W/m ² K)	28.60	28.61	8.81
Ra	1,74,395	1,90,964	2,91,419
Re	10,479	10,475	10,482
Nu_c	5.42	2.41	2.42
Nu_f	84.42	84.40	26.00

Table 3

Results for the typical configurations and operating conditions: case 3, selected coatings on the absorbing and bottom plates

Parameter	Type 1	Type 2	Type 3
η	0.6844	0.7194	0.6575
q_u (W/m ²)	547.55	575.48	526.03
T_c (K)	286.89	285.26	288.20
T_{ap} (K)	316.99	318.10	356.74
T_{bp} (K)	297.63	297.77	299.25
T_{fo} (K)	300.48	300.75	300.26
$h_{r,c-s}$ (W/m ² K)	48.50	318.29	30.69
$h_{r,ap-c}$ (W/m ² K)	0.31	0.31	0.38
$h_{c,ap-c}$ (W/m ² K)	1.86	0.83	0.88
$h_{r,ap-bp}$ (W/m ² K)	0.17	0.17	0.21
$h_{c,ap-f}$ (W/m ² K)	28.60	28.61	8.81
Ra	1,74,728	1,91,391	2,93,104
Re	10,479	10,475	10,482
Nu_c	5.43	2.41	2.42
Nu_f	84.42	84.40	26.00

299.4 K on the bottom plates, respectively, for type 1, type 2 and type 3 heaters. Nevertheless, it is found, from Table 3, that the use of selected coatings on both the absorbing plates and the bottom plates does not have any noticeable improvement on the thermal performances of all three types of heaters with respect to the Case 2, in which only the absorbing plates have selected coatings. However, the additional use of selected coatings on the glass covers is found, from Table 4, to be beneficial for the improvements of the thermal performances of all three types of heaters, although the improvements are not significant with only a further 2.18%, 1.24%, and 1.96% increase of efficiency, respectively, for type 1, type 2 and type 3 heaters with respect to the Case 2. On the other hand, the use of the selected coatings on the glass covers usually involve dramatical increases of costs

Table 4

Results for the typical configurations and operating conditions: Case 4, selected coatings on the absorbing plate, bottom plate and glass cover

Parameter	Type 1	Type 2	Type 3
η	0.7065	0.7318	0.6782
q_u (W/m ²)	565.17	585.46	542.56
T_c (K)	292.81	291.06	294.71
T_{ap} (K)	317.69	318.49	358.64
T_{bp} (K)	297.72	297.83	298.38
T_{fo} (K)	300.65	300.85	300.43
$h_{r,c-s}$ (W/m ² K)	0.86	1.03	0.75
$h_{r,ap-c}$ (W/m ² K)	0.17	0.16	0.20
$h_{c,ap-c}$ (W/m ² K)	1.75	0.83	0.89
$h_{r,ap-bp}$ (W/m ² K)	0.17	0.17	0.21
$h_{c,ap-f}$ (W/m ² K)	28.61	28.61	8.81
Ra	1,37,334	1,52,473	2,57,403
Re	10,477	10,474	10,480
Nu_c	5.06	2.41	2.42
Nu_f	84.40	84.39	26.00

and potential reductions of transmissivity of solar radiation through the glass covers, it is therefore not recommended.

In practical applications, it is more convenient to express the instantaneous efficiency of a heater in the following form:

$$\eta = F_R(\tau\alpha)_e - \frac{F_R U_L (T_{fi} - T_a)}{I}, \quad (29)$$

where F_R (dimensionless) is the heater heat-removal factor which relates the actual useful-energy gain of a heater to the useful gain if the whole heater surface were at the fluid's inlet temperature and its value is usually obtained from the $\eta \sim (T_{fi} - T_a)/I$ relation, U_L (W/m² K) is the heater's heat-transfer coefficient, and $(\tau\alpha)_e$ is the effective transmittance-absorptance product which is usually calculated by [1]

$$(\tau\alpha)_e \cong 1.01 \tau_c \alpha_{ap}, \quad (30)$$

where the factor "1.01" represents the averaged transmittance-absorptance product. The analytical solutions of η are plotted against $(T_{fi} - T_a)/I$ in Fig. 3, and the values of F_R and U_L for all three types of heaters in the four cases considered above are listed in Table 5. The results show that, for all cases considered, the values of the heater heat-removal factor F_R for Type 1 and Type 2 heaters are always larger than those for Type 3 heaters, confirming the above conclusion that the use of the cross-corrugated wavelike absorbing plate and bottom plate does significantly improve the thermal performance of a solar air-heater. The significant increases of F_R and the dramatic reductions of U_L in Cases 2, 3 and 4 with respect to Case 1 also give further support to the conclusions obtained above on the effect of selected coating.

Therefore, all the above results suggest that the use of selected coatings on the absorbing plates of all the heaters considered can substantially enhance the thermal performances of the heaters and therefore it is strongly recommended to be used in practical applications, whereas such a selected coating is not recommended for the bottom plates and the glass covers.

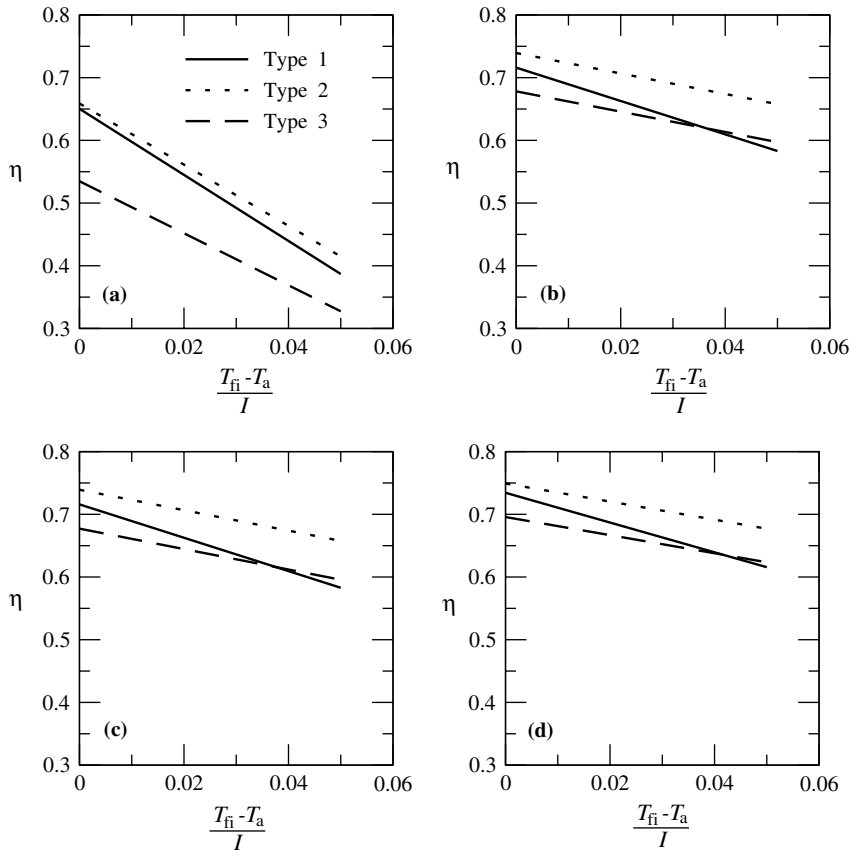


Fig. 3. Analytical solutions for efficiencies plotted against $(T_{fi}-T_a)/I$ for the four cases considered: (a) Case 1; (b) Case 2; (c) Case 3; and (d) Case 4.

3.3. Comparison between analytical solutions and experimental results

Two solar air-heaters were manufactured for this specific study. One of them belongs to type 1 heaters as described above with a cross-corrugated sine-wave shape absorbing plate and sine-wave shape bottom plate (referred to as the cross-corrugated heater). The other is a flat-plate solar air-heater which belongs to type 3 heaters as described above with both a flat absorbing-plate and flat bottom-plate (referred to as the flat-plate heater). Both heaters have a single glass-cover and a polyurethane-foam plate serving as the back insulation. The length and width of the heaters are 1.8 and 0.82 m, respectively. The glass cover has the thickness of 0.003 m and its transmissivity and absorptivity for solar radiation and the emissivity of thermal radiation are 0.84, 0.06 and 0.88, respectively. The polyurethane-foam-plate has an average thickness of 0.03 m and its thermal conductivity is 0.0346 W/mK. A black paint was used on the surfaces of the absorbing plate and the bottom plate, which has the absorptivity of solar radiation of 0.95 and the emissivity for thermal radiation of 0.95. The gap between the glass cover and the absorbing plate in the flat-plate heater has a thickness of 0.035 m while the average gap between the glass cover and the

Table 5
Analytical results of F_R and U_L for the four cases considered

Case	Type	F_R	U_L (W/m ² K)
Case 1	Type 1	0.807	6.530
	Type 2	0.817	5.971
	Type 3	0.664	6.247
Case 2	Type 1	0.888	2.995
	Type 2	0.917	1.780
	Type 3	0.841	1.926
Case 3	Type 1	0.888	2.995
	Type 2	0.917	1.780
	Type 3	0.840	1.938
Case 4	Type 1	0.911	2.608
	Type 2	0.930	1.553
	Type 3	0.863	1.673

sine-wave shape absorbing plate in the cross-corrugated heater has a thickness of 0.03 m. The gap between the absorbing plate and the bottom plate, which forms the air flow channel, in the flat-plate heater has a thickness of 0.06 m while the average gap between the sine-wave shape absorbing-plate and the sine-wave shape bottom-plate in the cross-corrugated heater has a thickness of 0.05 m. The wave amplitude and the wave length of both the sine-wave shape absorbing-plate and the sine-wave shape bottom-plate in the cross-corrugated heater are 0.0033 and 0.0314 m, respectively.

A series of experiments with different operating conditions were carried out. For the purpose of comparison, the experiments for the cross-corrugated heater and the flat-plate heater were under the same operating conditions. The experiments were carried out in accordance with the procedure stated in the methods for the testing of the thermal performances of solar air-collectors, which was designed by the Guangzhou Institute of Energy of China [20]. The solar-insolation rates incident on the heaters were measured by a TBQ-2 pyranometer and the temperatures at the output of the heaters and of the ambient environment were measured by thermocouples which were connected to a computer. Due to the limitation of the experimental conditions, measurements were only made for $T_{fi} = T_a$. To make comparisons between the analytical solutions and the experimental results, it is necessary to use the following expression for the instantaneous heater-efficiency [1],

$$\eta = F_0(\tau\alpha)_e - \frac{F_0 U_L (T_{fo} - T_a)}{I}, \quad (31)$$

where F_0 is a new heater heat-removal factor, which can be converted from F_R with the following relation [1],

$$F_0 = F_R \left(1 - \frac{A_c F_R U_L}{\dot{m}_f c_p} \right)^{-1}, \quad (32)$$

in which A_c (m²) is the area of the heater surface.

A series of analytical solutions were also obtained with the same values of the configurations and the operating conditions as those used in their corresponding experiments. The analytical and experimental results are presented in Fig. 4, where the experimental results are also found to support the above-mentioned conclusion, that is the use of the

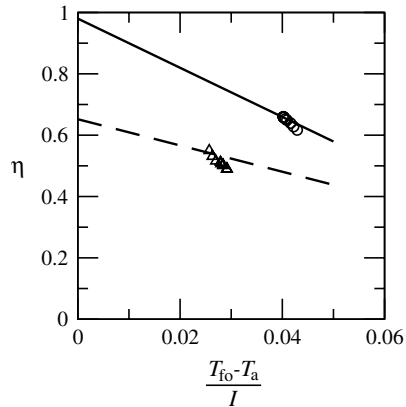


Fig. 4. Analytical solutions and experimental results of efficiencies plotted against $(T_{fo} - T_a)/I$. —, Type 1 heater, analytic solutions; ---, Type 3 heater, analytic solutions; \circ , Type 1 heater, experimental results; and \triangle , Type 3 heater, experimental results.

cross-corrugated wave-like absorbing plate and bottom plate does significantly improve the thermal performance of a solar air-heater, although the experimental results are found to be slightly lower than their analytical counterparts. It is believed that these discrepancies are mainly due to the very simple models used in the analytical solutions.

4. Conclusions

Analytical and experimental studies have been carried out on the thermal performance of cross-corrugated solar air-heaters for several configurations and operating conditions. These heaters consists of a wave-like absorbing-plate and a wave-like bottom-plate, which are crosswise positioned to form the air flow channel, with the aim of enhancing the turbulence and heat-transfer rate inside the air flow-channel which are crucial to the improvement of efficiencies of solar air-heaters. Two types of these heaters are considered. For the type 1 heater, the wave-like shape of the absorbing plate is along the flow direction and that of the bottom plate is perpendicular to the flow direction, while for the type 2 heater it is the wave-like shape of the bottom plate, that is along the flow direction and that of the absorbing plate is perpendicular to the flow direction. To quantify the achievable improvements with the cross-corrugated absorbing and bottom plates, a flat-plate solar air-heater which has both a flat absorbing-plate and a flat bottom-plate, is also considered. The results can be summarized as follows:

- Although the thermal performance of the type 2 heater is just slightly superior to that of the type 1 heater, both these cross-corrugated solar air heaters have a significantly superior thermal performance to that of the flat-plate one, with the achievable efficiencies of 58.9%, 60.3% and 48.6% for the type 1, type 2 and flat-plate solar air-heaters, respectively, under the typical configurations and operating conditions.
- The use of selected coatings on the absorbing plates of all the heaters considered can substantially enhance the thermal performances of the heaters and therefore its use is strongly recommended in practical applications, whereas such a selected coating is not recommended for the bottom plates and the glass covers.

- The experimental results also support the conclusion that the use of the cross-corrugated wave-like absorbing-plate and bottom-plate does significantly improve the thermal performance of a solar air heater, although the experimental results are found to be slightly lower than their analytical counterparts due to the very simple models used in the analytical solutions.

Acknowledgements

The financial support from The International Collaboration Scheme of Yunnan Province, the National Natural-Science Foundation of China (Grant No. 10262003), the Natural Science Foundation of Yunnan Province (Key Projects, Grant No. 2003E0004Z), and the Program for New Century Excellent Talents in the University of China (Grant No. NCET-04-0918) are gratefully acknowledged.

References

- [1] Duffie JA, Beckman WA. *Solar engineering of thermal processes*. 2nd ed. New York: Wiley; 1991.
- [2] Dickson WC, Chermisinoff PN. *Solar energy technology handbook*. New York: Marcel Dekker; 1980.
- [3] Williams JR. *Design and installation of solar heating and hot water systems*. New York: Ann Arbor Science Publishers; 1983.
- [4] Goldstein L, Sparrow EM. Experiments on the transfer characteristics of a corrugated fin and tube heat-exchanger configuration. *ASME J Heat Transf* 1976;98:26–34.
- [5] Goldstein L, Sparrow EM. Heat/mass transfer characteristics for flow in a corrugated wall channel. *ASME J Heat Transf* 1977;99:187–95.
- [6] Meyer BA, Mitchell JW, El-Wakil MM. Convective heat-transfer in Vee-trough linear concentrators. *Sol Energy* 1982;28:33–40.
- [7] Zhao XW, Li ZN. Numerical and experimental study on free convection in air layers with one surface V-corrugated. In: *Proceeding of the annual meeting of the Chinese Society of Solar Energy*, 1991; p. 182–92.
- [8] Stasiek JA. Experimental studies of heat transfer and fluid flow across corrugated-undulated heat-exchanger surfaces. *Int J Heat Mass Transf* 1998;41:899–914.
- [9] Piao Y. Natural, forced and mixed convection in a vertical cross-corrugated channel. M.Sc. thesis, The University of British Columbia, Canada; 1992.
- [10] Piao Y, Hauptmann EG, Iqbal M. Forced convective heat-transfer in cross-corrugated solar air heaters. *ASME J Sol Energy Eng* 1994;116:212–4.
- [11] Noorshahi S, Hall III CA, Glakpe EK. Natural convection in a corrugated enclosure with mixed boundary conditions. *ASME J Sol Energy Eng* 1996;118:50–7.
- [12] Gao WF. Analysis and performance of a solar air-heater with cross-corrugated absorber and back-plate, M.Sc. Thesis, Yunnan Normal University, China; 1996.
- [13] Gao WF, Lin WX, Lu ER. Numerical study on natural convection inside the channel between the flat-plate cover and sine-wave absorber of a cross-corrugated solar air-heater. *Eng Convers Manage* 2000;41:145–51.
- [14] McAdams WH. *Heat transmission*. 3rd ed. New York: McGraw-Hill; 1954.
- [15] Zhai XQ, Dai YJ, Wang RZ. Comparison of heating and natural ventilation in a solar house induced by two roof solar collectors. *App Therm Eng* 2005;25:741–57.
- [16] Swinbank WC. Long-wave radiation from clear skies. *Quart J Royal Meteorol Soc* 1963;89:339–48.
- [17] Hollands KGT, Unny TE, Raithby GD, Konicek LJ. Free convection heat transfer across inclined air layers. *ASME J Heat Transf* 1976;98:189–93.
- [18] Kays WM, Crawford ME. *Convective heat-and-mass transfer*. 2nd ed. New York: McGraw-Hill; 1980.
- [19] Weast RC, editor. *Handbook of tables for applied engineering science*. Boca Raton: CRC Press; 1970.
- [20] Li LD, Zhao XW. Studies on the methods of the testing of the thermal performances of solar air collectors. In: *Proceedings of the annual meeting of the Chinese Society of Solar Energy*, 1991; p. 149–55.